Microelectronic Engineering 86 (2009) 132–139

Contents lists available at ScienceDirect

Microelectronic Engineering

journal homepage: www.elsevier.com/locate/mee

Megasonic cleaning of wafers in electrolyte solutions: Possible role of electro-acoustic and cavitation effects

M. Keswani [a], S. Raghavan [a,*], P. Deymier [a], S. Verhaverbeke [b]

[a] Materials Science and Engineering, University of Arizona, 1235 East James E Rogers Way, Tucson, AZ 85721, United States
[b] Applied Materials Inc., Santa Clara, CA, United States

ARTICLE INFO

Article history:
Received 22 June 2008
Received in revised form 14 September 2008
Accepted 29 September 2008
Available online 17 October 2008

Keywords:
Wafer
Cleaning
Electrolyte
Megasonic
Electro-acoustic
Cavitation
Pressure amplitude

ABSTRACT

Investigations have been conducted on the feasibility of removal of particles from silicon wafers in electrolyte solutions of different ionic strengths irradiated with megasonic waves. Cleaning experiments have been performed using potassium chloride (KCl) as a model electrolyte and silica particles as model contaminant particles. Particle removal efficiency (PRE) increases with KCl concentration and transducer power density and much lower power densities may be used at higher KCl concentration for a comparable level of cleaning. Enhanced cleaning in KCl solutions has been explained as due to two types of electro-acoustic potentials, namely, ionic vibration potential (IVP) and colloidal vibration potential (CVP) that arise when the sound wave propagates through the electrolyte solution. Theoretical computations have shown that the removal forces due to CVP are much larger in magnitude than those due to IVP and are comparable to van der Waals adhesion forces.

The effect of ionic strength on cavitation has been investigated through the measurement of acoustic pressure in solutions using a hydrophone. Using Fourier transformation of time dependent pressure data, the size distribution of stable bubbles in KCl solutions of different concentration has been obtained.

1. Introduction

Wafer cleaning is a critical step in IC fabrication and it is estimated that over 50% of yield losses in semiconductor manufacturing are due to micro-contamination [1]. Not only is the number of cleaning steps increasing but also more critical requirements are being imposed by the International Technology Roadmap for Semiconductors (ITRS) on the tolerable size and quantity of particles on the wafer surface. ITRS roadmap dictates that the killer defect density, critical particle diameter and count to be 1.7×10^{-2} #/cm^2, 25.3 nm and 59.7 #/wafer, respectively for the front surface of a 300 mm wafer by the year 2009 [2].

Megasonic cleaning is routinely used in the semiconductor industry to remove particles from wafer and mask surfaces [3]. Cleaning is achieved through proper choice of chemical solutions, power density and frequency of acoustic field. Considerable work has been done on understanding particle removal mechanisms in megasonic cleaning using different solution chemistries. Bakhtaria et al. studied the removal of nano-particles from silicon wafers in SC-1 and DI water solutions [4]. They proposed a cleaning mechanism based on acoustic streaming for dislodging the particles and double layer repulsion force for preventing re-deposition of the particles. In another study, lifting, sliding and rolling of the particles resulting from higher ratio of drag force moment to adhesion force moment has been cited as responsible in megasonic cleaning of substrates [5]. Gale and Busnaina concluded that particles get removed from the wafer surface due to microstreaming and stable cavitation but are transferred to the bulk solution away from the wafer by means of acoustic streaming [6].

Although it is well known that propagation of sound wave through a dispersion of charged colloids in a medium containing ions results in an alternating electric field [7–12], effect of this field on removal of particles adhered to a substrate has not been investigated. There exist two mechanisms by which an electric field can be formed in a liquid medium irradiated with sonic waves, one requiring only the presence of ions and the other, charged colloids in conjunction with ions. The first one, described by Debye in 1933, is based on the difference in hydrated masses and frictional coefficients of the cations and the anions in the solution and leads to the formation of an oscillating potential known as ionic vibration potential (IVP) or Debye potential [7]. Measurements of IVP have been carried out in solutions of varying ionic strengths exposed to acoustic field of different intensities [8,9]. Potentials of the order of 0.3–10.2 μV have been measured for electrolytes such as lithium chloride (LiCl), sodium chloride (NaCl) and potassium chloride (KCl) in the concentration range of 10^{-5}–10^{0} M, at an ultrasonic frequency of 200 kHz and power density of 0.54 W/cm^2. A theoretical computation of electric field strength [7], E, and ionic vibration potential, ϕ, can also be made using Eqs. (1)–(3).

* Corresponding author.
E-mail address: srini@u.arizona.edu (S. Raghavan).

0167-9317/$ - see front matter © 2008 Elsevier B.V. All rights reserved.
doi:10.1016/j.mee.2008.09.042

$$E = \frac{\delta\phi}{\delta x} \tag{1}$$

where

$$\phi = \phi_0 e^{i(wt-kx)} \tag{2}$$

and

$$\phi_0 = cu_0 \frac{(4\Pi/Dw)\sum(\bar{n}_j m_j e_j/f_j)}{[1+((4\Pi/Dw)\sum(\bar{n}_j e_j^2/f_j))^2]^{0.5}} \tag{3}$$

In the above equation, ϕ_0 is the maximum amplitude of the potential, c is the speed of sound wave, u_0 is the maximum velocity of the solvent element, w is the frequency of the sound wave in rad/s, $\bar{n}_j$ is the number of ions of jth type per unit volume of solution in equilibrium condition, m_j, e_j, and f_j are the mass, charge and frictional coefficient of the jth ion, k is the ratio of frequency to speed of the sound wave and D is the dielectric constant of the medium.

When charged colloids are present in the ionic medium, the IVP is often accompanied by an electrokinetic effect that produces a potential termed as colloid vibration potential, CVP. This effect, first reported by Hermans and Rutgers [10–12], occurs due to the relative displacement between the particle and the surrounding ions in the double layer leading to formation of a dipole moment. The maximum value [13] of this dipole moment, m, can be estimated using the following equation:

$$m = \frac{6\pi v a \zeta \varepsilon_0 D}{w\left[1+\left(\frac{\alpha_0}{w\varepsilon_0 E}\right)^2\right]^{0.5}} f(\chi^a) \tag{4}$$

In Eq. (4), ε_0 is the permittivity of free space, ζ is the zeta potential of the particle, v is the maximum difference in velocity between the particle and the fluid, a is the particle radius, α_0 is the conductivity of the solution, w is the frequency of the sound wave in rad/s, $\frac{1}{\chi}$ is the double layer thickness, and $f(\chi^a)$ is a correction factor varying from 2/3 to 1 depending on the relative dimensions of double layer and particle radius.

In the case of particles adhered (stationary) to the wafer surface, the maximum difference in velocity between the particle and the fluid may be taken as the maximum velocity of the fluid, U, which is related to the transducer intensity, I, fluid density, ρ_l, and speed of sound in the medium, c, by Eq. (5).

$$U = \left(\frac{2I}{\rho_l c}\right)^{0.5} \tag{5}$$

As evident from Eqs. (4) and (5), the dipole moment increases with the transducer intensity, size and the zeta potential of the particle.

The relative motion between the particle and the surrounding ions causes the center of the charges in the double layer to become offset from its initial position. Due to the resulting offset between the centers of two charges, the particle experiences a net attractive force, F', to the displaced double layer ions in the direction of the offset. In an acoustic field, this force can be expected to oscillate and a simple model can be used to estimate the maximum amplitude of this force as [14]:

$$F' = \frac{mQ'}{l'^3} = \frac{Q'^2}{l'^2} \tag{6}$$

where Q' is the charge of the double layer that is displaced due to shift in the center of charges and l' is the offset between the center of particle and the double layer.

In a dilute colloidal suspension, microscopic potential developed around each colloid collectively forms the macroscopic potential, CVP. Experimentally determined values of CVP range from 0.4 to 1.7 mV per unit fluid velocity (cm/s) for silica dispersions (1–30 wt%) subjected to 0.2 MHz sound waves [15].

Additionally, acoustic properties of aqueous solutions such as bulk modulus, κ, and density, ρ_1, can be increased by 6% and 3%, respectively [16] by addition of electrolytes such as KCl at a concentration of 0.5 M. These increases, in turn, can increase the pressure amplitude, a, of the sound wave propagating through the medium by roughly 0.05 atm [17], according to Eq. (7).

$$a = (2I)^{0.5}(\rho_1\kappa)^{0.25} \tag{7}$$

It is well known that sound wave pressure amplitude can have a significant effect on the formation, growth and collapse of bubbles during cavitation. The theoretical work by Flynn and Walton et al. showed that the speed of the collapsing bubble increases two fold with an increase in pressure amplitude by 0.05 atm [18,19]. Young concluded that an increase in the sound pressure amplitude by 0.4 atm can transform a stable cavity to a transient cavity [20] and considerably affect the degree of cavitation in liquids.

Pressure amplitude measurements can be used to obtain useful information on the size distribution of stable cavities in the solution. When a stable bubble is driven at a frequency such that the ratio of driving frequency to resonance frequency is a rational fraction (i.e., w_d/w_r = n/m where n and m are integers), it can generate periodic motions which are subharmonics ($n = 1$, $m = 1,2,3\ldots$), harmonics ($m = 1$, $n = 1,2,3\ldots$) or ultraharmonics ($n = 2,3\ldots$, $m = 2,3\ldots$) of the driving frequency [21]. These periodic motions are reflected in the discrete Fourier transform (DFT) of the pressure amplitude data in the form of frequencies (w) of the oscillating stable bubbles in liquid of surface tension, σ, and density, ρ, which can be related to bubble sizes (R) using Eq. (8). This equation is based on the linear theory of small oscillations and considers that the relative changes in bubble volume during a bubble's expansion and contraction are small [20]. Assuming, that the contribution to the measured pressure amplitude from linear oscillations of bubbles is much higher than that from non-linear oscillations, Eq. (8) may be used to obtain stable bubble size distribution from the scattering of sound waves at different frequencies from these bubbles.

$$w^2 = \frac{1}{\rho R^2}\left[3\gamma\left(P_0 + \frac{2\sigma}{R}\right) - \frac{2\sigma}{R}\right] \tag{8}$$

where P_0 is the atmospheric pressure.

Although, stable cavities do not collapse violently, they often transform into transient cavities. It has been reported in literature that forces due to stable cavitation and associated microstreaming lead to dislodgement of particles from wafer surfaces [6].

In a semiconductor industry, megasonic cleaning of wafers is mostly carried out in alkaline solutions, which cause etching of the substrate. The work reported in this paper attempts to overcome this problem by using near neutral simple electrolyte solutions, by taking advantage of pressure and electrical effects induced by the propagation of megasonic field in solution.

2. Experimental procedures

Si (100) wafers (150 mm, p-type, 11–18 Ω cm) were used for cleaning experiments conducted in a class-10 clean room. Aminated and plain silica particles (Corpuscular Inc.) with a mean size of 392 ± 79 nm and 389 ± 108 nm, respectively were used as contaminating particles. Deionized water (18 MΩ cm), filtered through a 50 nm poly tetrafluoroethylene (PTFE) filter, was used to prepare all the experimental solutions.

A poly-vinylidene fluoride (PVDF) tank, donated by ProSys Inc., 25.4 cm × 25.4 cm × 29.8 cm in size, consisting of four rectangular transducers with a total area of 164 sq cm and operating frequency of 925 ± 25 kHz was used for megasonic exposure of the wafers. A

control unit was used to operate all the transducers simultaneously, resulting in a maximum power density of 2.17 W/cm^2.

The wafers were pre-cleaned in SC-1 ($1NH_4OH:1H_2O_2:50H_2O$) bath at 35 °C. A dispersion of contaminating particles was prepared in DI water and ultra-sonicated for 5 min at 40 kHz. The wafers were dipped in the dispersion at a pH of 5.9 and then spun at 1000 rpm for 1 min to deposit approximately 2500 particles. A particle count of less than 200 of unknown origin was present on the wafers prior to contamination. The wafers were cleaned, either in DI water or KCl solution, at 30 °C for 1 min. Particles on wafers were detected using SURFSCAN 5500.

The size distribution of contaminating particles in dispersion was measured using a Coulter N4 Plus particle analyzer. Zeta potential (ZP) of the particles was measured by Doppler electrophoretic light scattering technique using Coulter Delsa 440SX instrument. KCl was used as a base electrolyte to obtain the desired conductivity of solutions.

Hydrophone measurements were performed using a 2 mm needle shaped hydrophone (PVDF-Z44-1500 Onda Corp.) that tapered at the bottom to a pressure sensitive area with a diameter of about 1.5 mm. The total length of the hydrophone was approximately 2.5 inches. The hydrophone, located vertically about 8 inches from the transducers, was connected to a NI PCI-5102 scope, with the set-up designed to acquire 65,000 continuous samples for each run using LabVIEW 6.1. Sampling rate was 20 million samples/s. The output signal, in volts, from the oscilloscope was then converted to the Root Mean Square value (V_{RMS}) for comparison of results between different solutions. These RMS voltages were proportional to the pressure amplitude of the sound wave in the solution.

3. Results and discussion

3.1. Zeta potential measurements of plain and aminated silica particles

The zeta potential (ZP) of silica particles as a function of pH in solutions of different conductivities are displayed in Fig. 1. The isoelectric point (IEP) of plain silica and aminated silica particles was found to occur at pH values of 3.9, and 7.5, respectively. At the pH of ~6.0 used for particle deposition experiments, the ZP of plain and aminated silica particles were about −20 and + 45 mV, respectively in KCl solution of conductivity of 0.16 s/m (or ionic strength of 0.01 M). The ZP of aminated silica particles increased from 45 to 120 mV with decrease in solution conductivity from 0.16 to 0.001 s/m.

3.2. Megasonic removal of silica particles from wafer surfaces in potassium chloride solutions

In the first series of cleaning experiments, plain silica particles, characterized by a negative ZP at the deposition pH of 5.9, were used as contaminant. Wafers were cleaned in DI water and KCl solution of different concentrations at a megasonic power density of 0.077 W/cm^2. The results, shown in Fig. 2, indicate that in DI water alone, only 20% of the particles are removed. Addition of KCl does not improve cleaning efficiency until a critical KCl concentration is reached. By defining this critical concentration (C_c) as the concentration at which 50% particle removal efficiency (PRE) is achieved, for silica particles with negative ZP, C_c is about 0.05 M at a power density of 0.077 W/cm^2. A PRE of about 85% can be achieved in 0.5 M KCl. In the absence of a megasonic field, no removal of particles from the wafer surface was observed even in 1 M KCl solution.

Effect of power density on cleaning performance was investigated in both 0.5 M KCl solution and DI water. The results are shown in Fig. 3. As may be clearly seen from this figure, the removal of particles in KCl solution is significantly larger than in DI water at all power densities. The dependence of PRE on power density in KCl solution is not very significant beyond 0.073 W/cm^2. PREs greater than 90% can be achieved in KCl solutions.

Negatively charged silica particles are not expected to adhere very strongly to the silica surface, which is also negatively charged at a deposition pH of 5.9. This is evident from Fig. 3, where at power densities larger than 0.09 W/cm^2, the PRE is close to 90%. In order to investigate the removal of particles that may be strongly adhered to the wafer surface, a series of tests was performed using positively charged aminated silica particles (characterized by a positive ZP at the deposition pH). As shown in Fig. 4a, DI water alone exhibits a PRE of only 6% at 0.43 W/cm^2. Addition of KCl increases particle removal efficiency. A critical concentration of 3×10^{-5} M was observed at a power density of 0.43 W/cm^2. At a lower power density of 0.077 W/cm^2, C_c was calculated to be 0.2 M. The observed trend is that higher PREs are obtainable at lower power densities by increasing the KCl concentration.

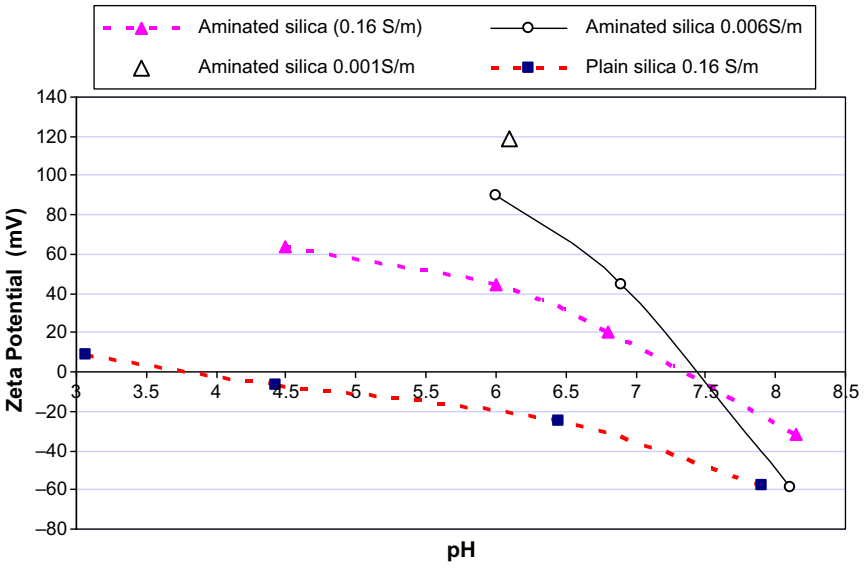

Fig. 1. ZP of plain and aminated silica particles.

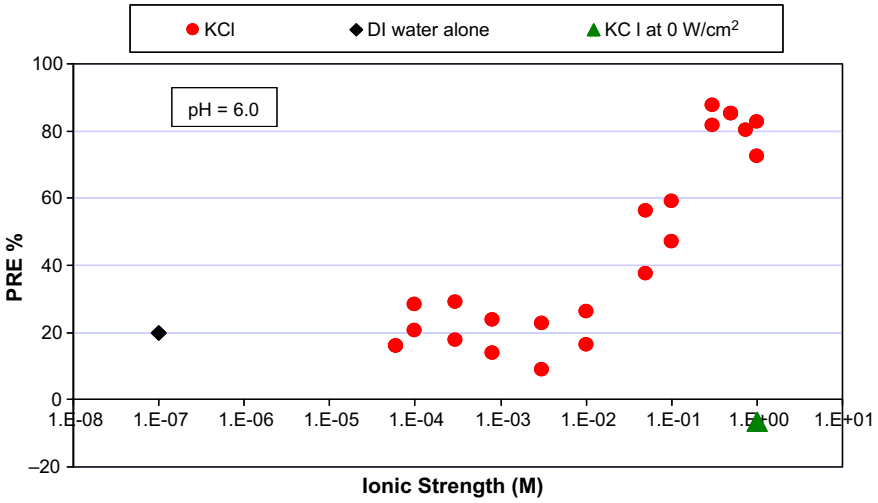

Fig. 2. Removal of plain silica particles from wafer surface in KCl solution of different concentrations at 30 °C and power density of 0.077 W/cm^2.

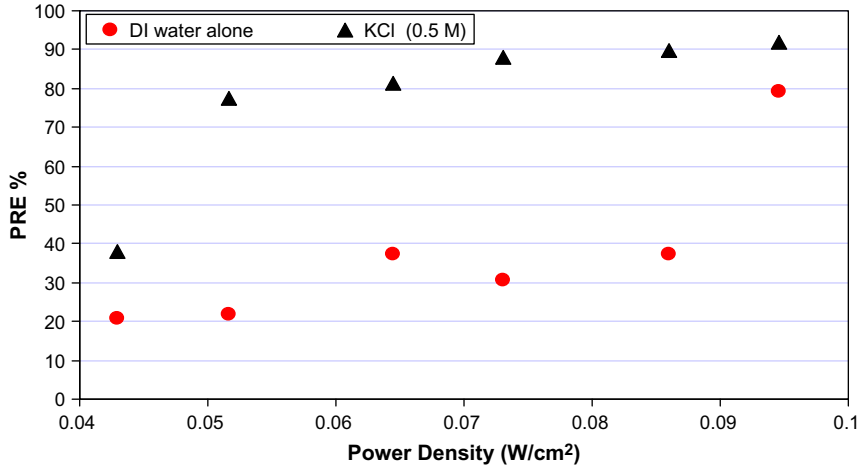

Fig. 3. Removal of plain silica particles from (chemical oxide covered) silicon wafer in 0.5 M KCl solution and DI water at 30 °C.

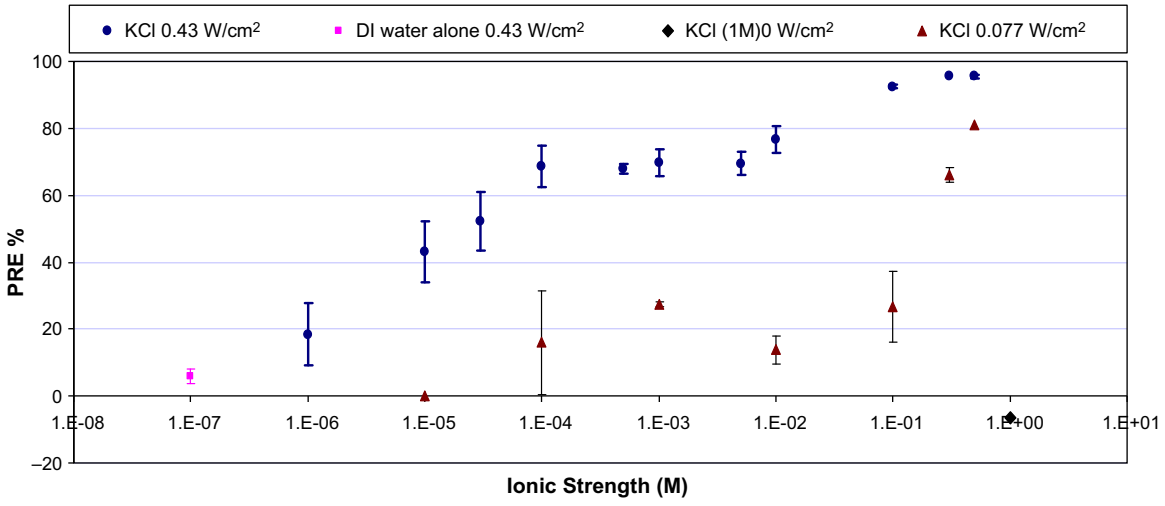

Fig. 4a. Removal of aminated silica particles from wafer surface in KCl solutions (pH of 6.0) at 30 °C.

The effect of megasonic power density on the removal of aminated silica particles from wafers immersed in 0.001 M KCl solution was also investigated. The values of PRE for different power densities are shown in Fig. 4b. At a lower power density of 0.077 W/cm^2, the removal of particles in KCl solution was about 30%. On increasing the power density to 0.43 W/cm^2, the PRE in-

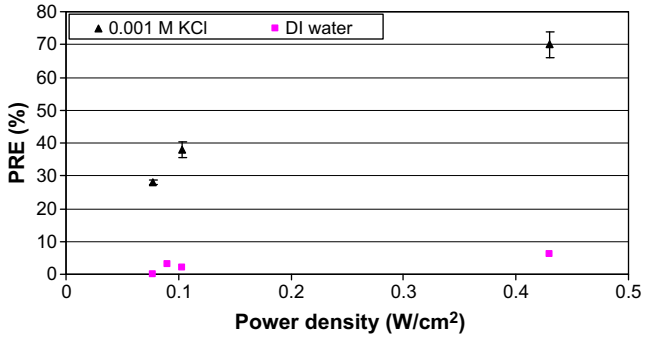

Fig. 4b. Removal of aminated silica particles from wafers immersed in 0.001 M KCl solution (pH of 6.0, $T = 30$ °C) at different megasonic power densities.

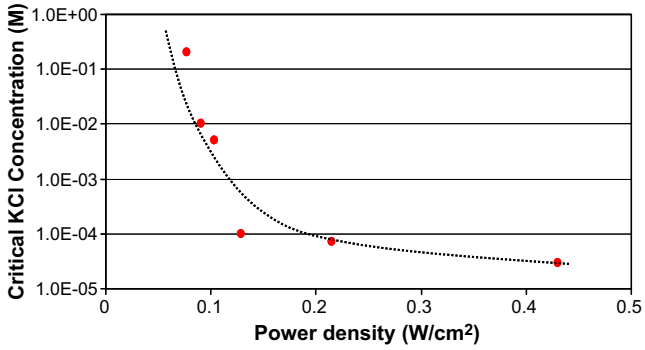

Fig. 5. Critical concentration of KCl at 30 °C for removal of aminated silica particles from wafer surface at different power densities.

creased to 70%. In the case of plain DI water, the PRE remained below 10% at all power densities $\leqslant$0.43 W/cm^2.

Critical concentrations of KCl at different power densities are plotted in Fig. 5 as a function of power density. It is clear that C_c increases with decreasing power density with the sharpest increase occurring at lower power density values.

3.3. Possible role of electro-acoustic effects on removal of silica particles from wafer surfaces

In order to understand the experimentally observed effect of enhanced removal of charged particles from wafer surfaces in ionic solutions irradiated with megasonic energy, forces on particles due to the electro-acoustic effects were calculated. As a first step in this direction, a theoretical computation of the effect of solution ionic strength and transducer intensity on the magnitude of Ionic Vibration Potential was performed. The maximum potential generated, ϕ_0, in KCl solutions of different concentrations at 25 °C and power densities ranging from 0.077 W/cm^2 to 2.17 W/cm^2 was calculated using Eq. (3). The frictional coefficients and the hydrated masses of the ions were obtained from [7] and [9], respectively. As displayed in Fig. 6, the potential increases with power density and KCl concentration, but saturates at 10^{-3} M KCl concentration. These values are consistent with experimentally measured values of IVP or Debye potential [9].

The force experienced by a charged particle with a specific charge density due to IVP is the product of charge density multiplied by the electric field due to IVP. Considering that IVP acts along a distance of $\lambda/2\pi$, the intensity of force is on the order of 10^{-15} N for a typical charge density of 2–10 μC/cm^2 on a particle in 10^{-3} M KCl solution, at a power density of 2.17 W/cm^2. For particle removal, force due to IVP should be larger than the van der Waals force of adhesion, which was calculated using Eq. (9).

$$F_v = \frac{A_{121} d_p}{12 z_0^2} \tag{9}$$

In this equation, d_p is the diameter of the particle, A_{121} is the effective Hamaker constant for particle–substrate interaction in water and z_0 is the distance of separation between the particle and the substrate. The value of A_{121} was estimated from Hamaker constants for silica (A_{11}: 6.0–6.5 $\times$ 10^{-20} J) and water (A_{22}: 4.4 $\times$ 10^{-20} J) [22]. Assuming 4 Å of separation distance [23,24] between the silica particle and the wafer surface, the van der Waals force was calculated to be 2–4 $\times$ 10^{-10} N, which is much larger than the estimated force on the particle due to IVP. Hence, it is difficult to explain the observed particle removal as due to the IVP generated due to megasonic field.

The next step was to compute the magnitude of force due to the formation of a dipole moment around the charged particle in an acoustic field. Initially, the force calculations were performed for a power intensity of 0.43 W/cm^2 and ionic strength of 10^{-4} M, which yielded PRE of 70% (for aminated silica particles). Since the particles are stationary (adhered to the wafer surface), v in Eq. (4) can be taken as the maximum velocity of the fluid, U, computed using Eq. (5). The dipole moment, m, computed using Eq. (4), was 3.8 $\times$ 10^{-24} cm. The calculation of force, F', requires Q' and l' which are not known. Different values of Q' were obtained by taking the ratio of m to l' for different values of l', as shown in Fig. 7.

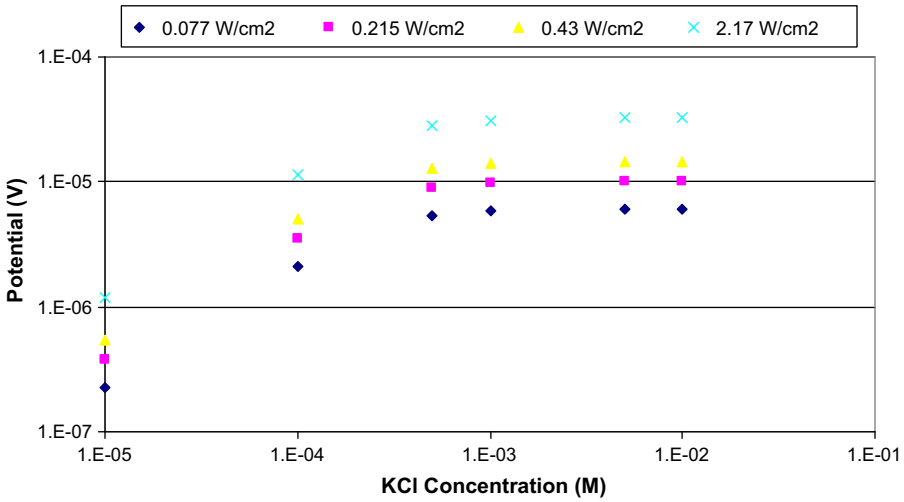

Fig. 6. IVP (Debye) potential in KCl solutions of different concentration and power densities.

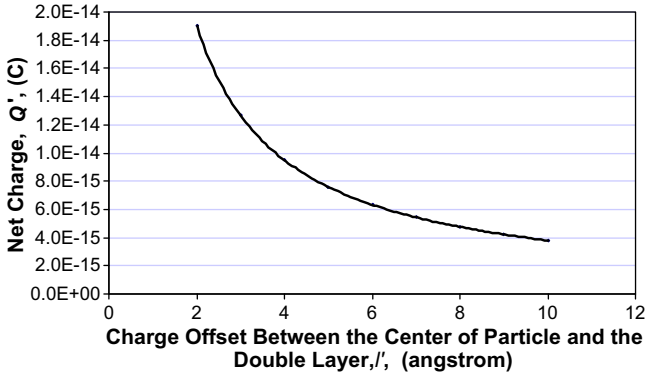

Fig. 7. Different combinations of Q' and l' that will satisfy a fixed value of dipole moment, m.

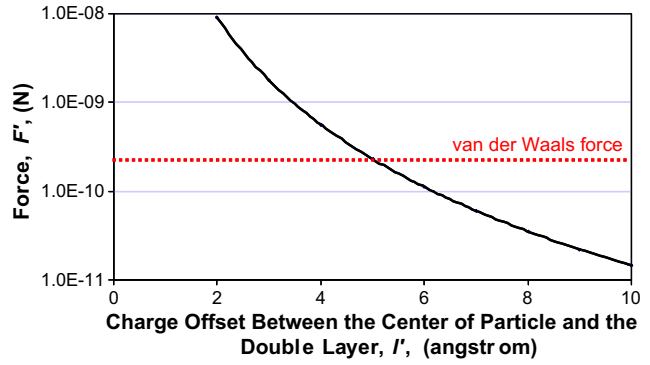

Fig. 8. Magnitude of removal force, F', computed for fixed m and different values of l', for transducer power density of 0.43 W/cm^2 and ionic strength of 10^{-4} M.

The force, F', computed for a fixed m and different value of l', is shown in Fig. 8. At net charge displacements lower than 1 nm, the removal force is comparable to the van der Waals adhesion force. These approximate calculations show that removal forces on the same order as adhesion forces can be produced in ionic solutions in conjunction with an acoustic field if the magnitude of the charge displacement has a favorable value.

3.4. Effect of ionic strength on removal force

The effect of ionic strength on removal force can be explained from the dependence of removal force, F', on charge Q' and charge offset l'. Assume a point center mass of charge $+Q$ surrounded by an ionic cloud of radius r' and charge $-Q$ at solution ionic strength I_1 as shown in Fig. 9 (left). In the absence of any acoustic field, the positive and negative charges are considered to act as though they are superimposed. The system has no dipole moment in this situation. When an acoustic field is applied, the center of the surrounding ionic charge becomes offset from its initial position by a distance l'; under this condition the net charge, Q', due to shift in the center of charges and the removal force, F', can be calculated using Eqs. (10) and (11), respectively [14].

$$Q' = Q\left(\frac{\frac{4}{3}\pi l'^3}{\frac{4}{3}\pi r'^3}\right) \tag{10}$$

$$F' = \frac{Q'^2}{l'^2} = \frac{Q^2 l'^4}{r'^6} \tag{11}$$

One can notice from Eq. (10) that Q' becomes equal to Q when l' attains a maximum achievable value of r' as shown in Fig. 9 (right).

Now, if the outer ionic cloud is compressed, say, due to an increase in solution ionic strength as shown in Fig. 10, the force F'' and charge Q'' for the same offset distance l' become:

$$Q'' = Q\left(\frac{\frac{4}{3}\pi l'^3}{\frac{4}{3}\pi r''^3}\right) \tag{12}$$

where r'' is the radius of the ionic atmosphere

$$F'' = \frac{Q''^2}{l'^2} = \frac{Q^2 l'^4}{r''^6} \tag{13}$$

Since, r'' is smaller than r', Q'' will be higher than Q' for constant l' and F'' will be greater than F'. However, with the compression of ionic cloud at higher ionic strength, I_2, the ions are distributed closer to the charged surface and therefore may experience higher electrostatic attraction which can reduce the value of offset, l'. Even for equivalent decrease in l' and r'', F'' will increase due to stronger dependency on r'' than l'. This indicates that the magnitude of removal force on the particle can increase with ionic strength.

3.5. Effect of ionic strength on stable cavitation

Cavitation phenomenon in solutions of different ionic strength was characterized by hydrophone pressure measurements from

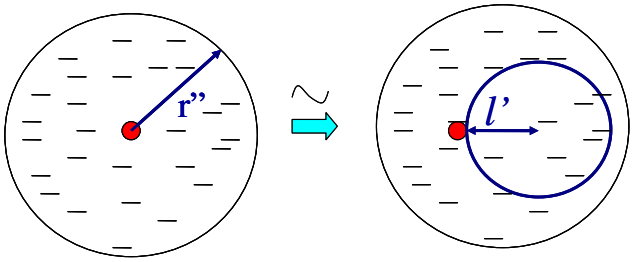

Fig. 10. Shifting of ionic charge at solution ionic strength I_2 ($I_2 > I_1$) in an acoustic field.

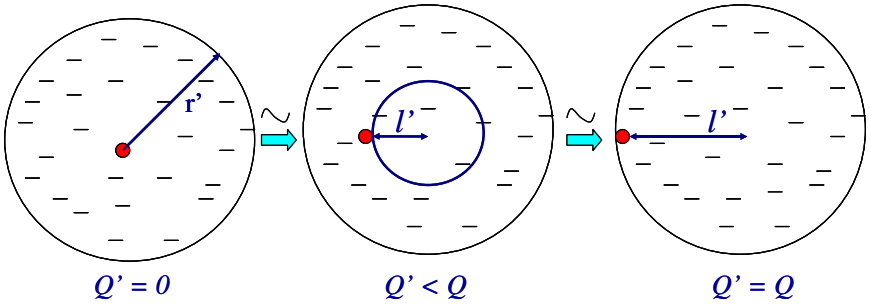

Fig. 9. Shifting of ionic charge in a solution of ionic strength I_1 due to applied acoustic field.

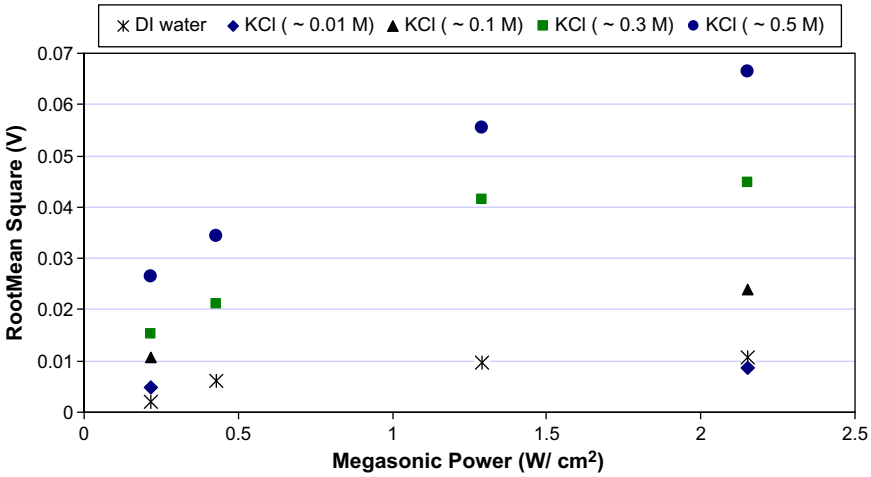

Fig. 11. Hydrophone measurements in KCl solutions of different concentration and power densities at 30 °C.

which information on size distribution of stable bubbles was extracted.

Signals from hydrophone were used to calculate root mean square voltage, V_{RMS}, which is an indicator of pressure amplitude in solutions. The results, shown in Fig. 11, demonstrate that the addition of KCl to DI water increases the pressure amplitude of the sound wave. The V_{RMS} values in DI water corresponded to a maximum pressure amplitude of approximately 1.66 atm and 2.33 atm at 0.43 W/cm^2 and 2.17 W/cm^2 respectively as measured using a calibrated HNR-1000 Onda Corporation hydrophone. The increase in pressure amplitude with the addition of KCl does not begin until a KCl concentration greater than 0.01 M is reached. At KCl concentrations equal to or lower than 0.01 M, it is possible that the bulk modulus and density of the KCl solution do not increase considerably so as to cause an increase in sound wave pressure amplitude. The difference in pressure amplitude between KCl solution and DI water also increases as the power density increases.

Discrete Fourier transform (DFT) of the pressure amplitude data was performed to obtain the distribution of frequencies of oscillating bubbles in solutions. Assuming the bubbles to be air bubbles, and assuming relative changes in bubble volume due to bubble expansion and contraction in response to the source pressure variations to be small, Eq. (8) from linear theory of small oscillations of a gas bubble was then used to obtain the bubble size distribution. The bubble size distribution in KCl solutions of different concentrations irradiated at 2.17 W/cm^2 is shown in Fig. 12. Since transient bubbles exist for less than one cycle, this bubble size distribution refers to that of stable bubbles in the system. It is clear from this figure that increasing KCl concentration increases the bubble sizes and also widens the distribution. In 0.01 M KCl solution, the bubble sizes span mainly from 1 to 10 microns. Bubbles of larger sizes start to appear with increase in KCl concentration. At 0.5 M KCl, bubbles as large a 100 μm are formed.

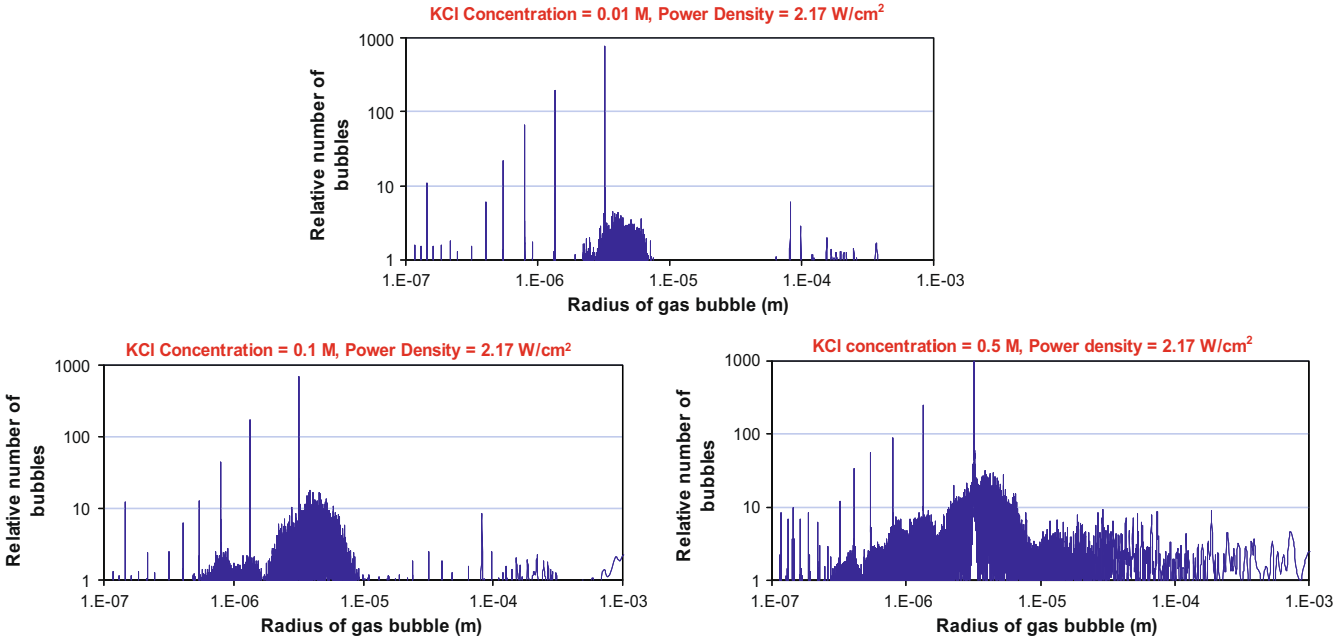

Fig. 12. Bubble size distribution in KCl solution of different concentrations at 30 °C and power density of 2.17 W/cm^2.

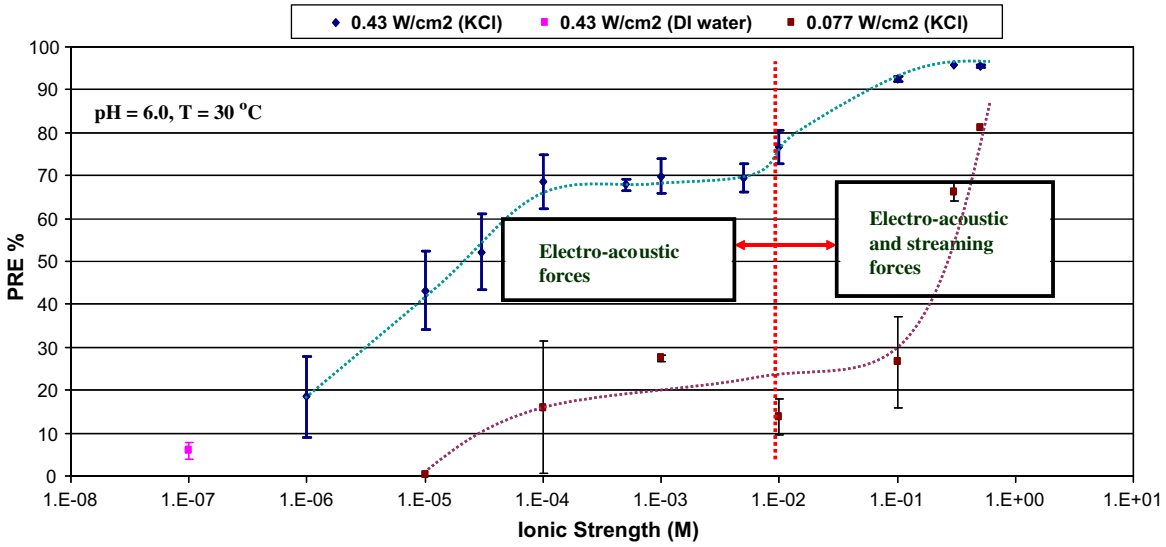

Fig. 13. Separation of electro-acoustic and streaming forces based on ionic strength of solution.

Data on the removal of silica particles presented in Fig. 4a is re-plotted in Fig. 13 to identify concentration regimes where electro-acoustic and cavitation forces may be operative.

Electro-acoustic forces are expected to be dominant at lower KCl concentrations. At concentration higher than 0.01 M, based on pressure data, forces due to cavitation and accompanying microstreaming cannot be ignored. For example, in the case of aminated silica particles, the increase in PRE from 20% to 75% with an increase in KCl concentration from 10^{-6} to 10^{-2} M at 0.43 W/cm^2 may be due to the electro-acoustic effect alone. A further increase in PRE to 95% in 0.5 M KCl can be expected to be a combined effect from electro-acoustic and cavitation forces. Similarly, the removal of aminated silica particles at lower power density of 0.077 W/cm^2 does not occur until a KCl concentrations greater than 0.01 M is reached. Since cavitation increases in KCl solutions with concentration greater than 0.01 M, the removal of particles can be expected to occur due to this effect.

4. Conclusions

Cleaning experiments have revealed that the removal of charged particles from wafer surfaces in a megasonic field can be significantly improved by employing electrolyte solutions of varying ionic strengths. Studies performed using KCl as an electrolyte showed that the removal of silica particles from SC1 treated silicon wafers was much higher in KCl solutions than in DI water at all megasonic power densities. The critical electrolyte concentration, C_c, for removal of particles was found to increase with a decrease in transducer power density. Theoretical computations showed that removal forces due to CVP were much larger in magnitude than those due to IVP and were comparable to van der Waals adhesion forces under certain conditions.

Hydrophone studies showed that the sound wave pressure amplitude can be increased in electrolyte solutions of ionic strengths greater than 0.01 M. Discrete Fourier transform (DFT) of pressure amplitude data in KCl solutions showed that higher pressure amplitude results in wider distribution of oscillating stable bubbles and therefore could provide additional force for removal of particles from wafers.

The key result from this work is that the removal particles can be achieved at lower acoustic power densities through the use of simple electrolyte solutions. Lower power density and near neutral solutions would enable damage free cleaning with lowered material loss per cleaning step, as mandated by ITRS roadmap.

References

[1] S. Wolf, R.N. Tauber, Silicon Processing for the VLSI Era, second ed., Process Technology, vol. 1, Lattice Press, 2000.
[2] ITRS, The International Technology Roadmap for Semiconductors, 2006.
[3] K. Muralidharan, M. Keswani, H. Shende, P. Deymier, S. Raghavan, F. Eschbach, A. Sengupta, Experimental and simulation investigations of acoustic cavitation in megasonic cleaning, in: Proceedings of SPIE, 65171E, 2007.
[4] K. Bakhtaria, R. Guldiken, P. Makaram, A. Busnaina, J. Park, Journal of The Electrochemical Society 153 (9) (2006) G846–G850.
[5] A. Busnaina, H. Lin, N. Moumen, IEEUSEMI Advanced Semiconductor Manufacturing Conference (2000) 328–333.
[6] G. Gale, A. Busnaina, Particulate Science and Technology 17 (3) (1999) 229–238.
[7] P. Debye, The Journal of Chemical Physics 1 (1933) 13–16.
[8] R. Zana, E. Yeager, The Journal of Physical Chemistry 71 (13) (1967) 521–535.
[9] S. Vidal, J. Simonin, P. Turq, The Journal of Physical Chemistry 99 (1995) 6733–6738.
[10] J. Hermans, Philosophical Magazine 25 (1938) 426.
[11] J. Hermans, Philosophical Magazine 25 (1938) 674.
[12] A. Rutgers, Physica 5 (1938) 46.
[13] B. Marlow, D. Fairhurst, H. Pendse, Langmuir 4 (1988) 611–626.
[14] D. Pollock, Physical Properties of Materials for Engineers, second ed., CRC Press, 1993. p. 502.
[15] E. Yeager, H. Dietrick, H. Hovorka, The Journal of the Acoustical Society of America 25 (3) (1953) 456–460.
[16] A. Kumar, Journal of Chemical and Engineering Data 48 (2003) 388–391.
[17] L. Spitzer, P. Bergmann, P. Frank, A. Yaspan, C. Herring, Physics of Sound in the Sea, Solar Analysis Group, 1945.
[18] H. Flynn, in: W. Mason (Ed.), Physical Acoustics, vol. 1B, Academic Press, 1964, p. 85 (Chapter 9).
[19] A. Walton, G. Reynolds, Advances in Physics 33 (1984) 595.
[20] F.R. Young, Cavitation, McGraw-Hill, London, 1989.
[21] W. Lauterborn, The Journal of the Acoustical Society of America 59 (1976) 283–293.
[22] H. Ackler, R. French, Y. Chiang, Journal of Colloid and Interface Science 179 (1996) 460–469.
[23] G. Kumar, S. Beaudoin, Journal of the Electrochemical Society 153 (2) (2006) G175–G181.
[24] L. Bergstrom, Advances in Colloid and Interface Science 70 (1) (1997) 125–169.